Current-phase relation in an intermediately coupled superconductor-superconductor junction

D. Agassi and J. R. Cullen
Naval Surface Warfare Center, White Oak Site, Silver Spring, Maryland 20903-5640
(Received 20 March 1996)

The limiting configuration of the S-N-S' junction in which the N-layer thickness is of the order of the screening length in metals ($\approx$1–2 Å) may serve as a model for a clean S-S' interface. This configuration supports one N-layer-attached gap state (manifold), with eigenenergy close to and less than the smaller superconducting gap. This gap state is interpreted as the excitation associated with breakage of interface-attached Cooper pairs, comprised of one electron from each side of the thin-N layer. The corresponding junction's current-phase (ψ) relation is calculated. The gap state is shown to contribute an appreciable ''sin(2ψ)'' correction term to the ''sin(ψ)'' Josephson term. The corresponding maximum-current magnetic-flux dependence of a two-junction configuration (SQUID) is predicted to have zeros shifted from their common loci at half-integer flux quanta.[S0163-1829(96)03738-1]

I. INTRODUCTION

In the no-coupling limit between two abutting superconductors (realized, e.g., by a thick insulating buffer layer), the arbitrary, spatially constant order-parameter phases of the two superconductors are obviously uncorrelated. As the superconductor-superconductor coupling increases, yet is ''weak,'' i.e., the electron transmission coefficient through the interface is small, Cooper-pairs tunneling becomes possible. The remarkable implication of such tunneling—the Josephson effect—is that the two superconductors' phases interlock such that their *difference* ψ across the buffer is determined by the junction's setup, e.g., the presence of an external magnetic field or a voltage. In the opposite limit of two ''strongly'' coupled superconductors (e.g., two abutting superconductors without a buffer layer), the combined system can be regarded as a composite superconductor, and hence cannot sustain a spatially varying phase. The objective of this work is to analyze an intermediate system, i.e., the coupling between the two superconductors is too strong to render pairs transport as tunneling, yet not sufficiently strong to eliminate a spatial phase variation. This physical regime is the intermediate coupling regime. Specifically, we analyze the S-δN-S' junction, where ''δN'' denotes a thin buffer layer, of thickness of order of the Thomas-Fermi screening length in metals, i.e., $k_F^{-1}\approx 1$ Å. This particular S-N-S' limiting configuration may provide a model for a ''clean'' S-S' interface, which is relevant to current transport in granular and layered superconductors.

When two dissimilar metals in equilibrium are brought into intimate contact, the formation of a δN layer is unavoidable.[1] To compensate for the two metals electron densities difference, excess electrons migrate across the metal-metal interface, thereby creating a thin depletion layer of the type encountered in semiconductor junctions.[2] This depletion layer acts as a *barrier* against additional charge flow between the two metals, and extends over a distance of the order of the Thomas-Fermi screening length. When the temperature of such a junction is sufficiently lowered, it transforms into a S-δN-S' junction. The δN barrier can be further augmented by judicious monolayer deposition during fabrication. The S and S' superconductors in such a junction are not weakly coupled since the buffer layer is atomically thin, yet, for a suitable δN barrier (see Sec. III), they are not sufficiently strongly coupled to preclude a phase difference at the interface.

This S-δN-S' junction, and its S-N-S' parent junction, were the subject of previous studies.[3–6] For the latter, discrete states in the N-layer with subgap energies were predicted by Andreev.[3] These gap states arise from a ''particle in a box'' situation in the N-layer, where a trapped electron undergoes multiple Andreev reflections off the two S-N walls. As the N-layer thickness shrinks to ''zero,'' as in the $N\rightarrow\delta N$ limiting configuration, the N-layer ''box'' is eliminated, yet *one* such subgap state survives.[5] This state is interface attached, localized in the direction normal to the junction's interface, and has a ψ-dependent eigenenergy. Since no confining ''box'' exists, this gap state is evanescent. Similar states arise under special surface-specific conditions. Examples are optical metal-air evanescent states, metal-dielectric surface plasmons, and gap states in specialized semiconductor-semiconductor interfaces.[7]

The key result of this work is the calculation of the S-δN-S' current phase relation $j(\psi)$, focusing on the gap state contribution. At zero temperature ($T=0$), and within the low incidence-angle approximation spelled out below,[8,9] the calculated current-phase relation is given to a good approximation by (see Sec. III)

$$\frac{j(\psi;T=0)}{j_{\mathrm{depair}}(T=0)}=a_1\sin(\psi)+a_2\sin(2\psi), \qquad (1.1)$$

where j_{depair} is the depairing current and the coefficients a_1, a_2 depend on the junction's parameters. For the parameter range considered here, $a_1\approx 0(.1)$ and $a_2/a_1\approx 1/3-1/4$ (see Table I). Expression (1.1) deviates from the standard Josephson junction expression[10a] in two respects, i.e., the critical current j_c is a sizable fraction of the depairing current, and the presence of a substantial second harmonic term $\sin(2\psi)$. This term is a consequence of the gap state (Sec. III).

Nonsinusoidal, intrinsic current-phase relations, such as is (1.1), are known for other types of junctions such as the

following. (1) A long, bridge-type, ''weak'' link.[11,12(a),13] (2) A finite-thickness S-N-S, and probably the S-N-I-N junctions,[8,9] have been inferred to have ''$\sin(n\psi)$'' terms (''n'' is an integer) in the current-phase relation.[4] Given the ''weak'' link nature of these junctions, we speculate that the higher harmonics terms in the current-phase relation are small. (3) A ''nonweak'' S-S'-S junction *near* T_c (Ref. 14) yields a current-phase relation reminiscent of (1.1) (compare Fig. 5 to Fig. 2 in Ref. 14). All these examples, however, differ either in the functional form or content from (1.1). In example (1), the nonsinusoidal current-phase relation is qualitatively different than (1.1). In example (2) the nonsinusoidal terms originate from ''particle-in-a-box'' gap states, which are qualitatively distinct from the evanescent state underlying (1.1). With regard to example (3), its current phase relation has been interpreted in terms of the proximity effect.[14] There is no room for the proximity effect in the S-δN-S' junction (self-consistency is discussed in the last section), and expression (1.1), which is a $T=0$ calculation, is attributed to the gap state. Nonsinusoidal current-phase relations may also originate from extrinsic sources, such as shorts and other junction imperfections. These, however, do not correspond to the ''clean'' configuration under study.

The presence of the second term in (1.1) suggests an experimental verification: the measurement of the interference of two such S-δN-S' junctions in a superconducting quantum interference device (SQUID) -ring configurations.[10(b)] The corresponding maximum-current magnetic-flux curves are calculated (Sec. IV). These curves show a characteristic distortion from the ''canonical'' SQUID curves[10(b),12(b)] which may serve as an experimental signature.

The paper is organized as follows. In preparation for the current calculations, Sec. II introduces the S-δN-S' junction model, the gap state eigenenergy is succinctly derived in a new representation and the gap state interpretation is discussed. Section III is devoted to the current-phase relation calculations. In the last section we present results for a two-junction ring configuration, or SQUID, discuss the validity of our model, briefly compare it with related work, and summarize the main results.

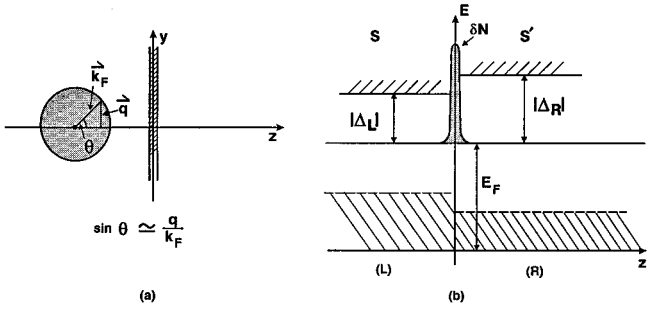

FIG. 1. Coordinates system and notations. (a) The chosen coordinates system and the δN buffer at $z=0$. The circle on the left represents the Fermi sphere, and the incidence-angle θ satisfies $\sin(\theta)\approx q/k_F$, where q is the transverse momentum, Eq. (2.2). (b) The energetics of the S-δN-S' junction model. The common Fermi energy, E_F, the gaps $|\Delta_L|$, $|\Delta_R|$, and the ''$U\delta(z)$'' potential are schematically depicted.

II. INTERFACE STATES

The analysis of the S-δN-S' junction is carried out in terms of the Fourier transformed Bogoliubov–de Gennes equations.[15] In the coordinate system defined in Fig. 1(a) and in the absence of electromagnetic fields the equations take the form

$$\begin{pmatrix} -\frac{\hbar^2}{2m}\frac{d^2}{dz^2}-E_F(q)-E+U\delta(z) & |\Delta(z)|e^{i\varphi(z)} \\ |\Delta(z)|e^{-i\varphi(z)} & \frac{\hbar^2}{2m}\frac{d^2}{dz^2}+E_F(q)-E-U\delta(z) \end{pmatrix}\begin{pmatrix} u(z) \\ v(z) \end{pmatrix}=(0), \tag{2.1}$$

where the symbols denote the following: The wave function $\Psi(\mathbf{r})$ in the Nambu representation and the Fermi energy associated with z-direction motion, $E_F(q)$, are

$$\Psi(\mathbf{r})=\begin{pmatrix} u(\mathbf{r}) \\ v(\mathbf{r}) \end{pmatrix}=\frac{1}{2\pi}\int d\mathbf{q}\, e^{i\mathbf{q}\cdot\boldsymbol{\rho}}\begin{pmatrix} u(z;\mathbf{q}) \\ v(z;\mathbf{q}) \end{pmatrix}, \quad \boldsymbol{\rho}=(x,y),$$

$$E_F(q)=\frac{\hbar^2k_F^2(q)}{2m}=E_F-\frac{\hbar^2q^2}{2m}=E_F\cos^2\theta\geqslant 0, \tag{2.2}$$

and the q dependence of $u(z;q)$, $v(z;q)$ in (2.1) has been suppressed. For simplicity, the bulk Fermi energy (and wave vector) E_F (and k_F) is assumed identical in the S and S' superconductors [Fig. 1(b)], $\mathbf{q}$ and θ denote the lateral momentum and angle of incidence, respectively, Fig. 1(a), and the electron mass is m. The δN layer is modeled as a ''$U\delta(z)$'' barrier (U of dimensions $[El]$), since the Thomas-Fermi screening length is considerably smaller than all other length scales in the system.[16,17,5] The gap function, $|\Delta(z)|\exp[i\varphi(z)]$, is assumed to vary only in the z direction, Fig. 1(b), and $E\geqslant 0$ is the excitation energy.

The boundary conditions across the δN interface at $z=0$, Fig. 1(b), are the continuity of the wave function and discontinuity of its first derivative

$$\left[\frac{d}{dz}\Psi(z;\mathbf{q})\bigg|_{z=\epsilon}-\frac{d}{dz}\Psi(z;\mathbf{q})\bigg|_{z=-\epsilon}\right]=\frac{2mU}{\hbar^2}\Psi(z=0;\mathbf{q}), \tag{2.3}$$

where $\epsilon\to 0$. The system's three dimensionality is reflected by the need to solve (2.1) for all $\mathbf{q}$ vectors satisfying

$E_F(q) \geqslant 0$. Except in $E_F(q)$, the $\mathbf{q}$ dependence is suppressed hereafter for the sake of notational conciseness.

To complete the model, the gap function $\Delta(z)$ profile has to be specified. The assumed profile is a z-coordinate step function, Fig. 1(b),

$$\Delta(z) = \theta(-z)|\Delta_L|e^{i\varphi_L} + \theta(z)|\Delta_R|e^{i\varphi_R}, \tag{2.4}$$

where φ_L and φ_R are the spatially-constant, arbitrary, phases of the S and S' superconductors, respectively.[5,6] Note that the φ_L and φ_R phases are assumed constant in *both* the z and y (transverse) directions. The legitimacy of (2.4) is discussed in the last section. The latter assumption implies a ''small'' junction.[12(c)] All in all the S-δN-S' model is characterized by three parameters,

$$\psi = \varphi_R - \varphi_L, \quad \delta = \left|\frac{\Delta_R}{\Delta_L}\right|, \quad K(q) = \left[1 + \frac{1}{2}\left(\frac{Uk_F(q)}{E_F(q)}\right)^2\right]^2. \tag{2.5}$$

Without loss of generality only $\delta > 1$ cases are considered [Fig. 1(b)], $\pi \geqslant \psi \geqslant -\pi$ since the φ's phases are specified modulus 2π, and $K(q) \geqslant 1$. According to the small incidence angle approximation discussed below, the latter's q dependence is neglected, i.e., $K(q) \approx K(0) \equiv K$.

The solutions of (2.1) are expanded in the following unnormalized ''electronlike'' ($\Psi^{(e)}$) and ''holelike'' ($\Psi^{(h)}$) basis functions[18,19]

$$\Psi^{(e)}_{\pm k^{(+)}}(z) = \begin{pmatrix} e^{i\varphi+\phi} \\ 1 \end{pmatrix} e^{\pm i k^{(+)} z},$$

$$\Psi^{(h)}_{\pm k^{(-)}}(z) = \begin{pmatrix} 1 \\ e^{-i\varphi+\phi} \end{pmatrix} e^{\pm i k^{(-)} z}, \tag{2.6}$$

where the amplitudes are expressed in terms of the unorthodox auxiliary variable ϕ:

$$\frac{E}{|\Delta|} = \cosh(\phi), \quad \frac{\Omega}{|\Delta|} = \sqrt{E^2 - |\Delta|^2} = \sinh(\phi) \tag{2.7a}$$

and the momenta $k^{(\pm)}$ are[16,19]

$$k^{(\pm)}(q) = \pm \frac{\sqrt{2m}}{\hbar} \sqrt{E_F(q) \pm \Omega}. \tag{2.7b}$$

For an eigenenergy larger than the gap, (2.7a) implies ϕ real and positive, while an eigenenergy in the gap implies a purely imaginary ϕ. The ''$\pm$'' signs in front of the square root symbol in (2.7b) are chosen such that ($\mathrm{Re}[k^{(\pm)}] \geqslant 0$, $\{\mathrm{Im}[k^{(+)}] \geqslant 0$, $\mathrm{Im}[k^{(-)}] \leqslant 0\}$), as required by the boundary conditions at $|z| \to \infty$. Note that for $E > |\Delta|$ extended states, $k^{(+)} > k_F(q)$ and $k^{(-)} < k_F(q)$, in keeping with the basis wave function (2.6) interpretation as ''electron'' and ''hole'' states. The added quotes signs around, e.g., ''electron,'' is a reminder that the electron and hole components in (2.6) are always admixed to some degree.

The method for solving (2.1) is outlined in Appendix A.[4,5,18] Two eigenfunction classes are obtained: extended states, where $E \geqslant |\Delta_L|$ (since by assumption $\delta > 1$) and localized gap states, with $E < |\Delta_L|$. In the representation (2.7a) the gap states eigenenergies are obtained from the solutions of the following two coupled equations for ϕ_L and ϕ_R:

$$\cos(\psi) = \cos(\tilde{\phi}_L)\cos(\tilde{\phi}_R) - \sqrt{K(q)}\sin(\tilde{\phi}_L)\sin(\tilde{\phi}_R),$$

$$\cos(\tilde{\phi}_L) = \delta\cos(\tilde{\phi}_R), \quad \phi_{L,R} = i\tilde{\phi}_{L,R}, \quad -\frac{\pi}{2} \leqslant \tilde{\phi}_{L,R} \leqslant \frac{\pi}{2}, \tag{2.8}$$

where the ''L,R'' indices refer to the ''left'' (S) and ''right'' (S') sides of the junction, respectively; see Fig. 1(b). The limiting cases where $(\delta,K) = (1,1)$, $(1,K)$, and $(\delta,1)$ (Refs. 5 and 6) follow trivially from (2.8).[20]

The structure of (2.8) implies several properties. (a) For each solution $\{\tilde{\phi}_L, \tilde{\phi}_R\}$ there is a degenerate solution $\{-\phi_L, -\tilde{\phi}_R\}$. Each state is a manifold: the q dependence of $K(q)$ implies that the eigenenergies form a *continuum*, extending from the eigenenergy corresponding to the $K = K(0)$ up to the bulk quasiparticle continuum threshold energy $|\Delta_L|$ (see below). The ensuing gap reduction is a manifestation of the ''weakened'' superconductivity in proximity to the δN buffer. (b) The $\psi \to -\psi$ transformation leaves the eigenenergy invariant. (c) Since $K(q) \geqslant 1$ and $|\cos(\psi)| \leqslant 1$, manipulations of (2.8) show that $\tilde{\phi}_L$ and $\tilde{\phi}_R$ have the same sign. Consequently, $\cos(\psi) - [\cos(\tilde{\phi}_L)]^2/\delta \leqslant 0$ and it follows that solutions to (2.8) exist only when[5]

$$\cos(\psi) \leqslant \frac{1}{\delta}. \tag{2.9}$$

Thus, barring the $\delta = 1$ singular case, a *finite* ψ (i.e., a finite current or magnetic field) is a prerequisite for the gap states to exist.

Although (2.8) can be solved in a closed form, its solutions are best discussed numerically. Figure 2(a) shows the K variation of the gap state energy for $\delta = 2$ and Fig. 2(b) is the δ variation of the gap state for $K = 40$ (the K-parameter range is discussed in the next section). As K increases, i.e., the δN barrier becomes less transparent, the eigenenergy is pushed up rapidly toward the quasiparticle continuum at $|\Delta_L|$, yet never reaches it. This trend is plausible, since in the $K \to \infty$ limit when the barrier decouples the two superconductors, no gap state exists.

The K variation in Fig. 2(a) mocks the q variation of $K(q)$ in (2.8). From (2.5) and Fig. 1(a), this variation is depicted in Fig. 3. This plot implies two properties: since only the $\theta \approx \pi/2$ angles (grazing angle incidence) are excluded in the low incidence angle approximation[8,9] [see text preceding (2.11), below], the ratio $\sqrt{(K(q)/K(0))}$ can attain arbitrarily large values. Hence a continuum of curves such as in Fig. 2(a) coexist. Secondly, the approximation $K(q) \approx K(0)$ is reasonable for a good fraction of incidence angles θ, as assumed in the small incidence angle approximation.

To gain insight into the content of the gap states (2.8), consider for simplicity the $K = 1$ limit, where no δN barrier exists. Following Appendix A, the corresponding two, unnormalized, degenerate gap states wave functions Ψ_1 and Ψ_2 are

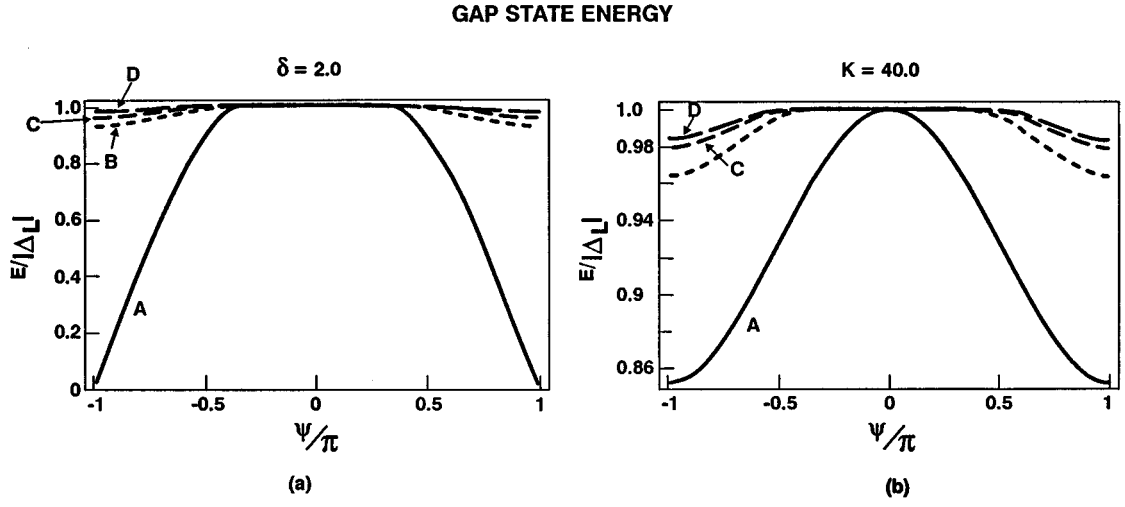

FIG. 2. Examples of calculated gap state eigenenergy, Eq. (2.8), as a function of ψ in its allowed domain, Eq. (2.9). (a) The K variation for a fixed $\delta=2$ case. The curves designation is $(A,B,C,D)=(K=1,\ K=20,\ K=40,\ K=80)$. (b) The δ variation for a fixed $K=40$ case. The curves designation is $(A,B,C,D)=(\delta=1,\ \delta=2,\ \delta=4,\ \delta=8)$.

$$\Psi_1(z):\quad \begin{pmatrix} e^{i[-\Psi+\tilde{\phi}_L(1)+\tilde{\phi}_R(1)]} \\ e^{i[-\varphi_R(1)+\tilde{\phi}_R(1)]} \end{pmatrix} e^{-ik_L^{(+)}z} \quad \text{for } z<0,$$
$$\begin{pmatrix} 1 \\ e^{i[-\varphi_R(1)+\tilde{\phi}_R(1)]} \end{pmatrix} e^{-ik_R^{(-)}z} \quad \text{for } z>0.$$

$$\Psi_2(z):\quad \begin{pmatrix} 1 \\ e^{i[-\varphi_L(2)+\tilde{\phi}_L(2)]} \end{pmatrix} e^{ik_L^{(-)}z} \quad \text{for } z<0,$$
$$\begin{pmatrix} e^{i[\psi+\tilde{\phi}_L(2)+\tilde{\phi}_R(2)]} \\ e^{i[-\varphi_L(2)+\tilde{\phi}_L(2)]} \end{pmatrix} e^{ik_R^{(+)}z} \quad \text{for } z>0. \tag{2.10}$$

The Ψ_1 state is ''electronlike'' on the left and ''holelike'' on the right side of the junction's interface and vice versa for the Ψ_2 state. This structure also follows for the S-N-S' junction gap states.[3,4] The latter, which are N-layer Andreev-reflected standing waves, fall into two classes: the first is comprised of a right-bound ''electron'' and left-bound ''hole'' in the N layer, and correspondingly an S'-bank decaying ''electron'' tail and an S-bank decaying ''hole'' tail. In the second class of gap states, the ''electron'' and ''hole'' roles are interchanged. As the N-layer thickness shrinks to zero, the N-layer portion of the wave functions is eliminated while the remaining decaying tails in the superconductors banks have precisely the structure (2.10). Thus these states owe their existence to an interface rather than to the presence of a well. Such evanescent states are encountered, e.g., in a metallic-dielectric interface (surface plasmons) and specialized semiconductor interfaces.[7]

The wave function (2.10) have *equal* amounts of electron and hole components [$u(z)$ and $v(z)$ components have equal magnitude]. This electron-hole admixture originates in the thin δN barrier and is distinct from that invoked by the bulk pairing interaction. Since bulk ''electron'' and ''hole'' states energies are, respectively, above and below the gap, it may not be surprising that an admixed state energy, such as (2.10), falls in the gap.

Further insight into the gap states (2.10) is obtained by considering the corresponding decay length, embodied in the $k^{(\pm)}$ momenta (2.7b). For this purpose, the square root in (2.7b) is customarily expanded to the zero order in the small parameter $\eta=|\Delta|/(E_F\cos^2\theta)\ll 1$. Since typically $|\Delta|/E_F\approx 10^{-4}$, 10^{-2} in low and high temperature superconductors, respectively, such an expansion is valid provided the $\theta\approx\pi/2$ incidence angles are excluded. This expansion is consistent with the $K(q)\approx K(0)=K$ approximation. The corresponding complex momenta $k^{(\pm)}$ (2.7b) are

$$k_{L,R}^{(\pm)}\cong \mathrm{sgn}(\tilde{\phi}_{L,R})k_F(q)\pm i\,\frac{|\sin(\tilde{\phi}_{L,R})|}{\pi\xi_{L,R}(q,T=0)},$$

$$\pi\xi_{L,R}(q;T=0)=\frac{\hbar^2k_F(q)}{m|\Delta_{L,R}|}\sim\frac{\hbar^2k_F(q=0)}{m|\Delta_{L,R}|}=\pi\xi_{L,R}(T=0), \tag{2.11}$$

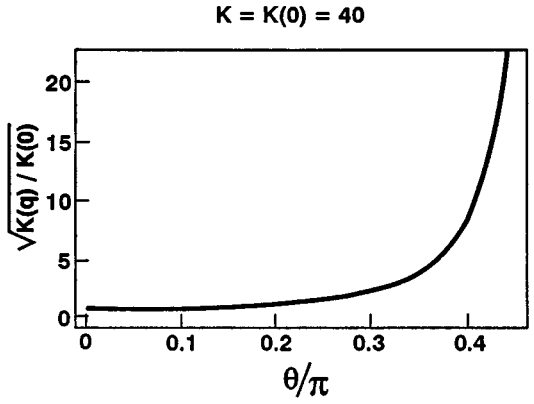

FIG. 3. The variation of $K(q)$, Eq. (2.5), with incidence angle θ, Fig. 1(a). The plotted curve is $[K(q)/K(0)]^{1/2}=[1+([(K(0))-1]/(\cos(\theta)^2)]^{1/2}/(K(0))^{1/2}$.

where $\xi_{L,R}(T=0)$ is the $T=0$ coherence length at the left and right sides of the junction,[10(c)] $\tilde{\phi}_{L,R}$ are the solutions of (2.8) and $k_F(q)/k_F(0)=\cos\theta$. Consequently, the gap state decay length $\Gamma\approx\pi\xi(T=0)/|\sin(\tilde{\phi})|$ is of the order of the coherence length, unless $|\sin(\tilde{\phi})|\ll 1$. (The latter is the case when the gap state is about to submerge into the bulk quasiparticle continuum.) This is interpreted to imply that the gap states are associated with interface-attached *Cooper pairs*. Such pairs are comprised of one electron from each side of the interface and hence, by a phase-space argument, are expected to be ''fragile'' in comparison to bulk Cooper pairs (with binding energy $|\Delta_L|$ or $|\Delta_R|$). This interpretation clarifies the prerequisite of a thin buffer layer (*considerably* smaller than the coherence length), to allow the formation of interface-attached ''mixed'' Cooper pairs. In standard *S-I-S* and *S-N-S* junctions the buffer layer is too thick to meet this prerequisite. This interpretation is also consistent with (2.9): it takes a finite current to break the mixed pairs.

Figure 4 shows the calculated $\tilde{\phi}$'s corresponding to one of the cases in Fig. 2(a). In conjunction with (2.11), this figure demonstrates that while the gap state energy varies by a relatively small amount, its decay length $\Gamma\approx\pi\xi(T=0)/|\sin(\tilde{\phi})|$ attains large ψ-modulated variations.

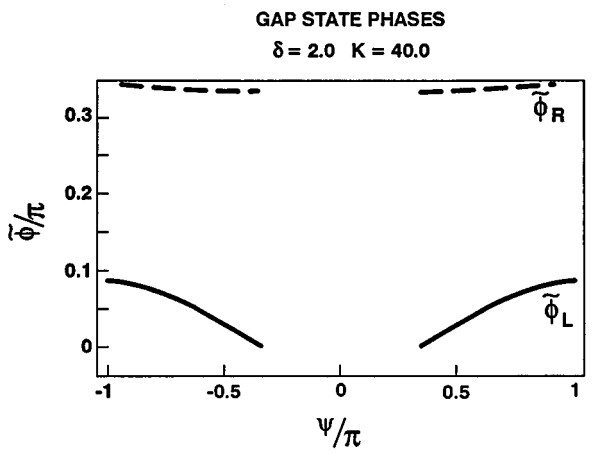

FIG. 4. An example of the calculated $\{\tilde{\phi}_L,\tilde{\phi}_R\}$, Eq. (2.8). The parameters are given in the heading.

III. CURRENT CALCULATIONS

The gap states (2.8) qualitatively distinguish the excitation spectrum of the S-δN-S' junction from that of an *S-I-S* junction, where such states are absent. Calculating the corresponding modified current-phase relation[10(a)] is the object of this section.

The calculation employs the Green function approach.[21,18] For the geometry of Fig. 1 and a $\Delta(z)$ profile, the current flows in the z direction. The corresponding expression is

$$j_z=C_0\int_0^{E_F}dE_F(q)\,\mathrm{Im}\left\{\sum_{\omega_n=-\infty}^{\infty}\int_0^{\infty}dz_1\int_{-\infty}^{0}dz_2\Delta(z_1)\Delta^*(z_2)\times G_\omega^{(0)}(z_1-z_2)G_{-\omega}(z_1,z_2)\right\},$$

$$C_0=-\frac{2|e|mk_BT}{\pi\hbar^3},$$

$$G_\omega(z,z')=\hbar\sum_{E_\alpha>0}\left[\frac{u_\alpha(z)u_\alpha^*(z')}{i\hbar\omega-E_\alpha}+\frac{v_\alpha^*(z)v_\alpha(z')}{i\hbar\omega+E_\alpha}\right], \tag{3.1}$$

where k_B and T are the Boltzmann constant and temperature, respectively, $\omega_n=(2n+1)\pi k_BT/\hbar$, $n=0,\pm1,\pm2,...$ are the Matsubara frequencies, and $G_\omega^{(0)}(z-z')$ and $G_\omega(z,z')$ are the diagonal and full Green functions, respectively, associated with (2.1) where $E\to E+i\omega_n$. The former is given in Appendix B while the latter is evaluated in terms of its spectral representation. By virtue of the Green functions symmetry properties

$$[G_\omega(z_1,z_2)]^*=G_{-\omega}(z_2,z_1),$$

$$[G_\omega^{(0)}(z_1,z_2)]^*=G_{-\omega}^{(0)}(z_2,z_1)=G_{-\omega}^{(0)}(z_1,z_2), \tag{3.2}$$

and the symmetrical distribution of the ω_n frequencies around $\omega=0$, simple manipulations of (3.1) yield that $j_z(\psi)=-j_z(-\psi)$, as it should. In the ''Born'' approximation, when $G_\omega(z,z')\approx G_\omega^{(0)}(z-z')$ and where the gap profile is (2.4), the Josephson relation $j_z=j_c\sin(\psi)$ [Refs. 10(a) and 21] follows. In the intermediate coupling regime, however, when higher order contributions become important, deviation from this simple current-phase relation is expected.

To simplify the calculation of (3.1), two approximations are introduced. First, we limit ourselves to the $T\to0$ limit, where the ω_n summation is well approximated by an integral. Secondly, the Green function and wave functions are calculated in the small incidence-angle approximation, i.e., the q-dependent quantities $K(q)$ [Eq. (2.5)] and $k^{(\pm)}(q)$ [Eq. (2.11)] are replaced by their $q=0$ values.[8,9] This approximation is expected to yield an *upper limit* to the current for the following reason. The contribution to the z-directed current from $\theta>0$ scattering events is expected to be smaller than that of the $\theta=0$ scattering event. Hence, in the approximation where all scattering events (designated by **q**) are treated as a $\theta=0$ scattering event, the summed result is obviously an overestimate. Also, since grazing-angle scattering events ($\theta\approx\pi/2$) are primarily specular reflection, their contribution to the z-directed current is expected to be small, in support of the above approximation. While only a full calculation can quantitatively assess the validity of these arguments, the additional weak θ dependence of $K(q)$, Fig. 3, and $k_F(q)/k_F(0)=\cos\theta$ ($\sin\theta\approx q/k_F$) further support the small-θ approximation.

Applying the above approximations and employing the calculated wave functions (Appendix A) in (3.1) yields a current expression of the form

$$\frac{j_z(\psi,\delta,K;T=0)}{j_{\mathrm{depair}}(T=0)}=r_B(\psi,\delta,K)+r_S(\psi,\delta,K),$$

$$j_{\mathrm{depair}}(T=0)=-\frac{2}{3\pi^2}\frac{m|e|E_F\sqrt{|\Delta_L\Delta_R|}}{\hbar^3}, \tag{3.3}$$

where the complicated, dimensionless, r_B and r_S terms denote the contributions of the gap (localized) and scattering

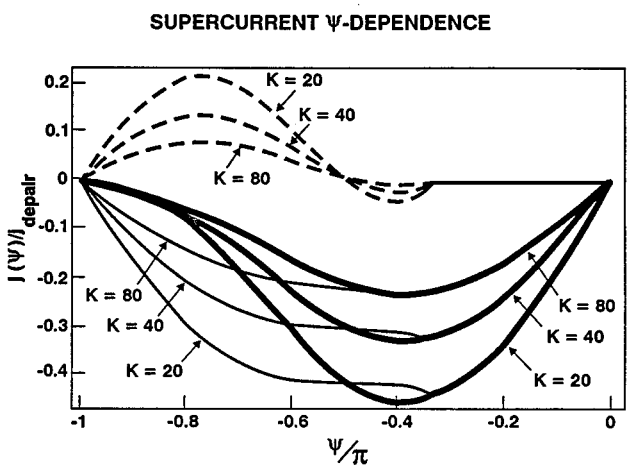

FIG. 5. Variation of the relative current with K, Eq. (3.3). The broken line, thin solid line, and a bold solid line denote r_B, r_S, and their sum, respectively. The r_B contribution exists only for ψ values satisfying (2.9). As discussed in the text, the approximations invoked imply that this calculation overestimates the current.

(delocalized) excited states to the current, and $j_{\text{depair}}(T=0)$ is the geometrical mean of the S and S' depairing currents densities.[10(d)] The latter follows since the bulk depairing current is $j_{\text{depair}}^{(\text{bulk})}(T=0)=-|e|n_e v_S(T=0)$ with $n_e=k_F^3/(3\pi^2)$ and $v_S=\Delta(T=0)/(\hbar k_F)$. Since the two superconducting banks are assumed to have the same E_F, Fig. 1(b), expression (3.3) for $j_{\text{depair}}(T=0)$ ensues.

Before presenting the results, consider the ''realistic'' range of the K (or U) parameter. For this purpose, the ''$U\delta(z)$'' barrier in (2.1) is estimated by equating it to the barrier of a clean metal-metal interface. In the latter, the barrier is determined by difference in the electrostatics, exchange and correlation energies across the dissimilar metals interface. Lang and Kohn[1] calculations for a metallic surface indicate that the effective single electron potential extends over half a Fermi wavelength from the surface, and is of the order of 1 eV. Assuming, as a rough estimate, that the presence of another metal only slightly alters these quantities, U can be extracted from the calculations in Ref. 1. We find that $U=8.3r_s^{-1}$ eV Å, where $n=4\pi r_S^3/3$ is the electron density (for dissimilar metals interface, the smaller of the two U values should be chosen). In particular, for a Pb/Al interface this gives $U\approx 7.5$ eV Å. Combining this with typical metallic values,[22] $k_F\approx 1.7$ Å^{-1}, $E_F\approx 10$ eV yields form (2.5) $K=K(0)=3.3$. This is a lower limit estimate, since deviation from an ideally clean interface augments the barrier. Note also that $K(q)\simeq U^4$, and is q dependent; see Fig. 3. The latter property and uncertainties in U imply that typical values of the K parameter are considerably larger. Unequal Fermi energies of S and S' superconductors will further augment the effective K value.

Representative results of the calculations are shown in Fig. 5. In the relevant ψ domain, the $r_B(\psi)$ component is *not* negligible, and $r_S(\psi)$ and $r_B(\psi)$ are qualitatively distinct: while $r_S(\psi)$ has no nodes, reminiscent of a ''$\sin(\psi)$'' curve, the $r_B(\psi)$ component has one node, reminiscent of a ''$\sin(2\psi)$'' curve. The opposite sign of $r_B(\psi)$ and $r_S(\psi)$ terms reflects the depletion of the scattering states strength by the gap state. Other characteristics are the large magnitude of the junction's critical current—a sizable fraction of the depairing current, the asymmetry with respect to $\psi/\pi=-0.5$, and the approximate overall down-scaling as $K^{-1/2}$ with the barrier strength parameter K. The sizable critical current reflects the intermediate coupling regime in the system under study. On the other hand, a ''large'' critical current may imply non-negligible self-consistency gap corrections. This important point is discussed in the next section. The current down-scaling trend with increasing K reflects the approach to the weak coupling regime as the barrier height increases.

TABLE I. Total relative-current best fit [Eq. (3.3)].

δ	K	a_1	a_2	a_3
2	20	0.39	0.13	−0.026
2	40	0.28	0.087	−0.012
2	80	0.21	0.056	−0.006
1.2	100	0.24	−0.001	0.010
4	80	0.18	0.053	−0.010

The above results and the expectation of a ''$\sin(n\psi)$ harmonics'' in S-N-S' suggests the following parametrization of (3.3) [Eq. (1.1)]:

$$\frac{j(\psi,\delta,K;T=0)}{j_{\text{depair}}(T=0)}=a_1\sin(\psi)+a_2\sin(2\psi)+a_3\sin(3\psi), \tag{3.4}$$

where the coefficients are fitted to the calculated curves. Table I shows the results for several representative examples. The corresponding fits, not shown here, are excellent. As Table I shows, the dominant correction to the leading ''$\sin\psi$'' term is a ''$\sin(2\psi)$'' component, with an appreciable amplitude $a_2/a_1\approx 0.25-0.3$ for all the examples considered. In view of the $r_B(\psi)$ curve's shape in Fig. 5, the ''$\sin(2\psi)$'' term in (3.4) originates primarily from the gap state.

IV. DISCUSSION AND SUMMARY

The appreciable ''$\sin(2\psi)$'' term in the current-phase relation (3.4) can be tested experimentally by measuring the interference of two such junctions in a ring configuration, i.e., a generic SQUID device.[10(b),12(b),23] The characteristics of the corresponding maximum-current-density magnetic-flux dependence can be assessed by the following argument. Consider two types of SQUIDS, i.e., a standard SQUID where only the ''$\sin(\psi)$'' term contributes, and a hypothetical SQUID where only the ''$\sin(2\psi)$'' term contributes. The corresponding maximum-current-density magnetic-flux curves, denoted by $j_{\max}^{(1)}(\Phi)$ and $j_{\max}^{(2)}(\Phi)$, are[10(b)]

$$\frac{j_{\max}^{(1)}(\Phi)}{2j_c}=\left|\cos\left(\frac{\pi\Phi}{\Phi_0}\right)\right|,\quad \frac{j_{\max}^{(2)}(\Phi)}{2j_c}=\left|\cos\left(\frac{2\pi\Phi}{\Phi_0}\right)\right|, \tag{4.1}$$

where Φ is the magnetic flux through the ring and $\Phi_0=\pi\hbar c/|e|=1630$ (eV Å)$^{1/2}$ is the flux quantum. Note that $j_{\max}^{(1)}(\Phi)$ and $j_{\max}^{(2)}(\Phi)$ vanish at $\Phi/\Phi_0=\pm 0.5,\pm 1.5,...$ and at $\Phi/\Phi_0=\pm 0.25,\pm 0.75,\pm 1.25,...$, respectively. Consequently, for a current-phase relation which is a mixture of the above

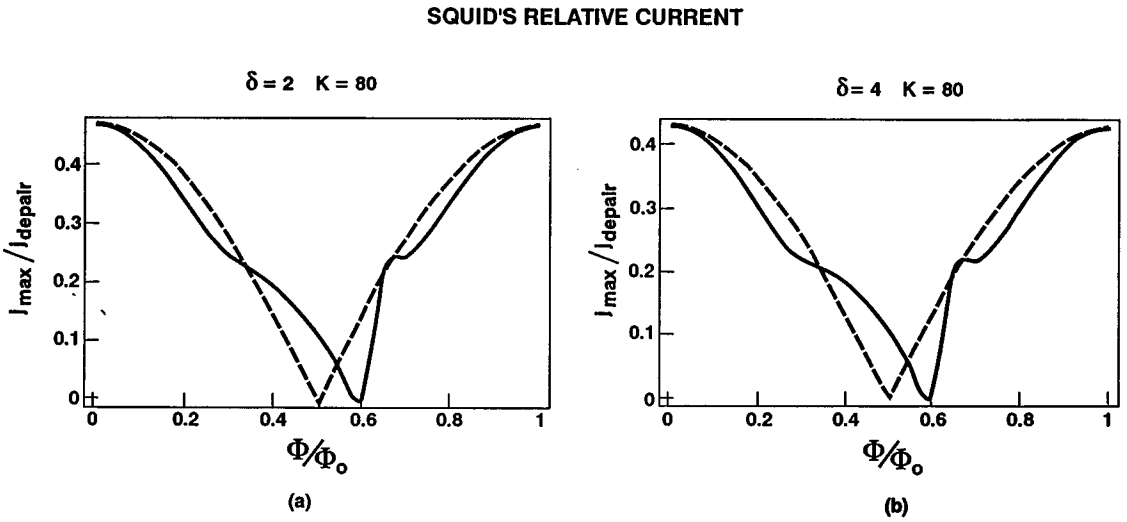

FIG. 6. Two examples of SQUID calculations; see Table I. The solid line is $|j_{\max}(\Phi)/(2j_{\text{depair}})|$, where $j(\psi)$ is given by the fitted form (3.4) and the extremum calculation follows Ref. 10(b). The fluxes Φ and Φ_0 are defined in text; see after Eq. (4.1). The broken line is the standard Josephson junction result, $|\cos(\pi\Phi/\Phi_0)|$, normalized to coincide with the solid line at $\Phi=0$. The parameters of each example are indicated in the headings.

two ψ dependencies, as (3.4) is, the ensuing $j_{\max}(\Phi)$ curve is a coherent mixture of $j^{(1)}_{\max}(\Phi)$ and $j^{(2)}_{\max}(\Phi)$.

Utilizing the parametrization (3.4), the calculation for two cases of Table I are presented in Fig. 6. As the above consideration indicates, the curve's zero is shifted from the conventional location at $\Phi/\Phi_0=0.5$, with distortions on both sides of the $\Phi/\Phi_0=0.5$ point. These signatures may be amenable to an experimental measurement. At higher temperatures we conjecture that the bound state contribution will be smeared out, and a sinusoidal current phase relation ensues. Consequently, the distortions calculated in Fig. 6 will disappear.

Next consider the validity of the present model and approximations. The assumed phase profile (2.4) implies a constant [in the x,y axes, Fig. 1(a)] phase discontinuity ψ. The latter corresponds to a ''small'' junction assumption,[12(c)] i.e., $L<\lambda_J$, where L is the junction's transverse dimension and λ_J is the Josephson penetration length. In this limit the longitudinal current nonuniformity is minimal, i.e., ψ is a constant. To realize this situation in the intermediate coupling regime, note that[10(e)] $\lambda_J=[(c\Phi_0)/(8(\pi^2)j_c(2\lambda_L+d))]^{1/2}$, where j_c is the junction's critical current density, λ_L is the London penetration depth, and ''d'' is the δN layer thickness. Adopting the values $\lambda_L\approx1000$ Å, $d\approx0$ Å, from Fig. 5 $j_c(T=0)\approx0.1j_{\text{depair}}(T=0)$, $E_F=1$ eV, $\Delta_L\approx\Delta_R=0.002$ eV, $\hbar c=1970$ eV Å it follows from (3.3) that $j_c(T=0)\approx2.0\times10^7$ A/cm^2 and $\lambda_J\approx2000$ Å. Thus, with modern deposition techniques, making a ''small'' S-δN-S' junction is feasible, as well as enhancing the δN barrier with judicious monolayer deposition.

As Fig. 5 shows, the critical current is a sizable fraction of the depairing current, which raises the consistency question of the of the assumed steplike gap profile (2.4). Self-consistent gap calculations have been carried out for the related S-N,[8,9,19,24,25] S-I,[25] and S-N-S configurations.[26] These studies show that the self-consistent gap profile is rounded at the interface. For S-N at $T=0$,[8] however, the rounding is minimal. At a finite temperature $T/T_c\approx0.5$, the extension of the rounding increases and is of the order of the N-layer thickness.[25,26] These calculations imply that in our case, of an *atomically* thick N layer and at $T=0$, the step-shaped gap profile (2.4) is a reasonable approximation. In a related consideration, our calculations invoke the small-incidence angle approximation [θ in Fig. 1(a)]. As noted in Sec. II, this implies that the calculated current is an overestimate. Therefore, the ''true'' currents are probably smaller than calculated here, which lends additional support to the validity of the steplike gap profile (2.4). A quantitative examination of this issue is deferred to another publication.

The present work complements other microscopic calculations of the S-N-S and S-Sm-S junctions (Sm denotes a semiconductor) (Refs. 17 and 27) and related configurations.[28] The former focuses on configurations where the two banks have the same gap [$\delta=1$, Eq. (2.5)] and the ''N'' or ''Sm'' width is finite and delineated by two δ barriers. All temperatures are considered. By comparison, this work considers an asymmetric configuration, containing one δ barrier and only $T=0$. One consequence of the difference in configurations is that here only a ''single,'' evanescent state exists (disregarding the lateral momentum dependence; see Sec. II) provided that ψ is large *and* $\delta>1$ [Eq. (2.9) and Fig. 2(b)]. By comparison, the gap states in Refs. 3, 4, 27, and 28 form sequence, which exists for all ψ values. As Fig. 5 shows, for $\delta>1$ the current curve is skewed toward angles $\psi<|\pi/2|$ since at these angles the bound state does not contribute while at larger angles it suppresses the scattering states contribution. In the limit when $\delta=1$, where the bound state exists for all ψ values [Fig. 2(b)], the ensuing current curve is a flattened, symmetric ''sin'' curve (not shown). These results are qualitatively different from those in Ref. 27, where the current curve is skewed toward angles $\psi>|\pi/2|$.

It is instructive to briefly compare the S-δN-S' gap states, Eq. (2.8), to other gap states in superconductor layered structures. As mentioned above, unlike ''particle-in-a-box'' gap states in the S-N-S' junction, the present gap states are evanescent states of Cooper pairs, of the type encountered, e.g., in optics. Gap states were recently predicted for a high temperature superconductors junction with a $d_{x^2-y^2}$ gap symmetry,[29] in superconductor-ferromagnetic and in superconductor-paramagnetic junctions.[30] These gap states have a different origin; the former emanates from the gap's sign change along nodal lines and the latter invokes a spin flip mechanism. Both these aspects are absent in the model considered above.

In summary, we discussed the gap state manifold in an S-δN-S' junction model, where ''δN'' is an atomically thin interface layer modeled by a ''$U\delta(z)$'' barrier. This barrier represents all atomically-thick impediments at a ''clean'' interface, such as the electronic depletion layer. The electron transmission coefficient across this thin barrier is large, hence the coupling between the S and S' banks is ''intermediate'' (nonweak). For the sake of simplicity, the Fermi energies of the S and S' banks are assumed equal. Unequal Fermi energies have the effect of augmenting the effective interface barrier.

The gap state represent a broken ''mixed'' Cooper pair, i.e., a pair where each electron resides on either side of the thin buffer layer. The gap state manifold are localized in the direction normal to the interface plane, with a ψ-dependent decay length that exceeds the coherence length under certain conditions.

Two implications of the gap state presence are calculated, i.e., the junction's supercurrent-phase relation $j(\psi)$, and the maximum-current magnetic-flux dependence in a ring (SQUID) configuration, comprised of two, parallel S-δN-S' junctions. The $j(\psi)$ functional dependence deviates from the Josephson junction expression, $j=j_c\sin(\psi)$, by the presence of an appreciable ''$\sin(2\psi)$'' term, and j_c is a fraction of the depairing current. The former is a direct consequence of the gap states while the latter manifests the intermediate coupling regime. For a two, parallel S-δN-S' ring configuration (SQUID) we find that the maximum-current flux dependence deviates from the standard two S-I-S ring configuration dependence by a shift in the curve's zeros and its skewness. This prediction calls for an experimental test.

ACKNOWLEDGMENT

We acknowledge the support of the NSWC-Carderock Division In-house Laboratory Independent Research (ILIR) program.

APPENDIX A: OUTLINE OF SOLUTION OF (2.1)

For each eigenenergy there are four degenerate states.[18,19] These correspond to an ''electron'' or ''hole'' approaching from the left and the right sides of the junction. In terms of (2.6), the corresponding wave functions are

$$
\begin{aligned}
(e\Rightarrow):\quad & z<0 \quad (\Psi^{(e)})_{k_L^{(+)}}+A(\Psi^{(e)})_{-k_L^{(+)}}+B(\Psi^{(h)})_{k_L^{(-)}},\\
& z>0 \quad C(\Psi^{(e)})_{k_R^{(+)}}+D(\Psi^{(h)})_{-k_R^{(-)}},\\
(h\Rightarrow):\quad & z<0 \quad (\Psi^{(h)})_{-k_L^{(-)}}+A(\Psi^{(e)})_{-k_L^{(+)}}+B(\Psi^{(h)})_{k_L^{(-)}},\\
& z>0 \quad C(\Psi^{(e)})_{k_R^{(+)}}+D(\Psi^{(h)})_{-k_R^{(-)}},\\
(\Rightarrow e):\quad & z<0 \quad A(\Psi^{(e)})_{-k_L^{(+)}}+B(\Psi^{(h)})_{k_L^{(-)}},\\
& z>0 \quad (\Psi^{(e)})_{-k_R^{(+)}}+C(\Psi^{(e)})_{k_R^{(+)}}+D(\Psi^{(h)})_{-k_L^{(-)}},\\
(\Leftarrow h):\quad & z<0 \quad A(\Psi^{(e)})_{-k_L^{(+)}}+B(\Psi^{(h)})_{k_L^{(-)}},\\
& z>0 \quad (\Psi^{(h)})_{k_R^{(-)}}+C(\Psi^{(e)})_{k_R^{(+)}}+D(\Psi^{(h)})_{-k_R^{(-)}},
\end{aligned}
\tag{A1}
$$

with self-explanatory notation. The coefficients are obtained by matching the wave functions and first derivatives, [Eq. (2.3)], at the interface. Similarly, the gap states are obtained by omitting the source term in (A1).

Considering the gap states in the $U=0$ limit is instructive. Lengthy algebra yields the exact dispersion relation

$$
\begin{aligned}
&(k_L^{(+)}-k_R^{(-)})(k_L^{(-)}-k_R^{(+)})(1-e^{2\phi_L})(1-e^{2\phi_R})\\
&\quad+(k_L^{(+)}+k_L^{(-)})(k_R^{(+)}+k_R^{(-)})(1-e^{-i\psi+\phi_L+\phi_R})\\
&\quad\times(1-e^{i\psi+\phi_L+\phi_R})=0,
\end{aligned}
\tag{A2}
$$

where the symbols are defined in (2.5) and (2.7). The $k^{(\pm)}$-dependent factors in the two terms in (A2) differ vastly when $\eta=|\Delta|/[2E_F(q)]\ll 1$: according to (2.11), the $k^{(\pm)}$ momenta difference is of the order $[K_F(q)|\Delta|]/E_F(q)$ while the $k^{(\pm)}$ momenta sum is of the order $2k_F(q)$. Thus the ratio of the $k^{(\pm)}$ factors in the two terms in (A2) is of the order $\eta=(|\Delta|/[2E_F(q)])^2$. Hence, to the order η^2, the second term in (A2) must vanish, i.e., the $k^{(\pm)}$-independent factors must be set to zero. This yields Eq. (2.8). To the lowest order of η, the scattering states $(e\Rightarrow)$ and $(\Leftarrow h)$ entail $A=D=0$, while the $(h\Rightarrow)$, $(\Leftarrow e)$ states entail $B=C=0$.

APPENDIX B: UNPERTURBED GREEN FUNCTION FOR δ POTENTIAL

The Matsubara Green function pertaining to the diagonal parts of (2.1), $G_\omega^{(0)}(z,z')$, satisfies

$$
\left[\frac{\hbar^2}{2m}\frac{d^2}{dz^2}-U\delta(z)+E_F(q)+i\hbar\omega\right]G_\omega^{(0)}(z,z')=\hbar\,\delta(z-z'),
\tag{B1}
$$

with the boundary conditions of decaying at $|z-z'|\to\infty$. Equation (B1) is readily solved by summation of the corresponding Dyson series

$$
G_\omega^0=g_\omega^{(0)}+g_\omega^{(0)}Vg_\omega^{(0)}+g_\omega^{(0)}Vg_\omega^{(0)}Vg_\omega^{(0)}+\cdots,
\tag{B2}
$$

where

$$g_\omega^{(0)}(z-z')=\left[-\frac{im}{\hbar k_\omega}\right]e^{ik_\omega|z-z'|},\quad V=U\delta(z),$$

$$k_\omega=\pm\left(\frac{2m}{\hbar^2}[E_F(q)+i\hbar\omega]\right)^{1/2}$$

$$\cong \mathrm{sgn}(\omega)k_F(q)+i|\omega|\left(\frac{m}{2E_F(q)}\right)^{1/2}. \tag{B3}$$

The ''±'' sign in (B3) is chosen such that $\mathrm{Im}(k_\omega)>0$, to abide by the boundary conditions at infinity. The closed form summation of (B2) is

$$G_\omega^{(0)}(z,z')=g_\omega^{(0)}(z-z')+R_\omega g_\omega^{(0)}(z)g_\omega^{(0)}(z'),$$

$$R_\omega=\frac{U/\hbar}{1-g_\omega^{(0)}(0)(U/\hbar)}. \tag{B4}$$

The relevant section of (B4) under the integral sign in (3.1) is of the form

$$G_\omega^{(0)}(z_1<0,z_2>0)=\frac{g_\omega^{(0)}(z_1-z_2)}{1-\epsilon_\omega}, \tag{B5}$$

$$\epsilon_\omega=-\frac{\mathrm{sgn}(\omega)imU}{\hbar\sqrt{2mE_F(q)}},$$

which manifestly shows that $G_\omega^{(0)}(z_1,z_2)\to 0$ as $U\to\infty$, i.e., the inability of current to cross an infinite strength δ barrier.[21]

[1] N. D. Lang and W. Kohn, Phys. Rev. B **1**, 4555 (1970).

[2] J. P. McKelvey, *Solid State and Semiconductor Physics* (Harper International, New York, 1969), Chap. 13.

[3] A. F. Andreev, Sov. Phys. JETP **22**, 455 (1966).

[4] I. O. Kulik, JETP **30**, 944 (1970).

[5] S. V. Kuplevakhskii and I. I. Falko, Sov. J. Low Temp. Phys. **17**, 501 (1991).

[6] A. Furusaki and M. Tsukuda, Phys. Rev. B **43**, 10 164 (1991); A. Furusaki and M. Tsukuda, Physica B **165&166**, 967 (1990).

[7] O. A. Pankratov, S. V. Pakhomov, and B. A. Volkov, Solid State Commun. **61**, 93 (1987); D. Agassi, Appl. Phys. Lett. **51**, 2227 (1987); D. Agassi and V. Korenman, Phys. Rev. B **37**, 10 095 (1988).

[8] W. L. McMillan, Phys. Rev. **175**, 537 (1968); **175**, 559 (1968).

[9] G. B. Arnold, Phys. Rev. B **18**, 1076 (1978).

[10] M. Tinkham, *Introduction to Superconductivity* (Krieger, Malabar, FL, 1985), (a) Chap. 6, (b) p. 202–203, (c) p. 65, (d) p. 119, (e) p. 200.

[11] I. O. Kulick and A. N. Omelyanchuk, Sov. J. Low Temp. Phys. **4**, 142 (1978).

[12] A. Barone and G. Paterno, *Physics and Applications of the Josephson Effect* (Wiley-Interscience, New York, 1982), (a) pp. 184–185, (b) Sec. 12.3, (c) p. 70.

[13] L. D. Jackel, R. A. Buhrman, and W. W. Webb, Phys. Rev. B **10**, 2782 (1974); L. D. Jackel, J. M. Warlaumont, T. D. Clark, J. C. Brown, and R. A. Buhrman, Appl. Phys. Lett. **28**, 353 (1976); L. D. Jackel, W. H. Henkeis, J. M. Warlaumont, and R. A. Buhrman, Appl. Phys. Lett. **29**, 214 (1976).

[14] A. Baratoff, J. A. Blackburn, and B. B. Schwartz, Phys. Rev. Lett. **25**, 1096 (1970).

[15] P. G. De Gennes, *Superconductivity of Metals and Alloys* (Benjamin, New York, 1966), p. 140.

[16] G. E. Blonder, M. Tinkham, and T. M. Klapwijk, Phys. Rev. B **25**, 4515 (1982).

[17] U. Schussler and R. Kummel, Phys. Rev. B **47**, 2754 (1993).

[18] A. Furusaki and M. Tsukuda, Solid State Commun. **78**, 299 (1991).

[19] Chr. Bruder, Phys. Rev. B **41**, 4017 (1990).

[20] To convert the results here to those in Ref. 5, set $T(t)=2/[1+\sqrt{(K)}]$, where $T(t)$ is in the Ref. 5 notation.

[21] I. O. Kulik and I. K. Yanson, *The Josephson Effect in Superconductive Tunneling Structures* (Israel Program for Scientific Translations, Jerusalem, 1992), Chap. 2.

[22] N. W. Ashcroft and N. D. Mermin, *Solid State Physics* (Holt, Rinehart and Winston, New York, 1976), p. 38.

[23] F. Bloch, Phys. Rev. B **2**, 109 (1970).

[24] O. Entin-Wohlman, J. Low Temp. Phys. **27**, 777 (1977).

[25] Y. Tanaka and M. Tsukada, Phys. Rev. B **42**, 2066 (1990).

[26] Y. Tanaka and M. Tsukada, Phys. Rev. B **47**, 287 (1993); Y. Tanaka, H. Yamagami, and M. Tsukuda, Solid State Commun. **79**, 349 (1991).

[27] U. Gunsenheimer, U. Schussler, and R. Kummel, Phys. Rev. B **49**, 6111 (1994).

[28] G. B. Arnold, J. Low Temp. Phys. **59**, 143 (1985); **68**, 1 (1987).

[29] J. H. Xu, J. L. Shen, J. H. Miller, Jr., and C. S. Ting, Phys. Rev. B **50**, 16 762 (1994); C. R. Hu, Phys. Rev. Lett. **72**, 1526 (1994); J. Yang and C. H. Hu, Phys. Rev. B **50**, 16 766 (1994).

[30] S. V. Kuplevakhskii and I. I. Falko, Physica C **235–240**, 3247 (1994); **235–240**, 2345 (1994).